Assessing High-Resolution SkySat Imagery and Deep Learning for Detection of Coconut Scale Insect Outbreaks in the Philippines

David Joshua R. Santos[1], Harry Casimir Merida[1], Ara Joy Abatayo[1]

[1]Geospectrum Marketing Services, Pasig City, Philippines - david.santos@geospectrum.com.ph, harrycasimeri2012@gmail.com, arajoyabatayo@gmail.com

Keywords: Cocolisap, DETReg, Object Detection, High Resolution Imagery, Visible Atmospherically Resistant Index.

Abstract

Coconut scale insect (CSI; *Aspidiotus rigidus*) outbreaks cause canopy chlorosis and tree mortality, posing a serious threat to coconut-based livelihoods in the Philippines. This study assesses the potential of high-resolution SkySat imagery (0.5 m) combined with the DETReg deep-learning object detection model to automatically identify CSI-affected coconut crowns. Two outbreak sites were examined: Anahawan, Southern Leyte, and the Philippine Coconut Authority–Zamboanga Research Center (PCA-ZRC) in Talisayan, Zamboanga City. SkySat ortho analytic surface reflectance scenes were processed in ArcGIS Pro and QGIS to generate false-color composites and compute the Visible Atmospherically Resistant Index (VARI). A training dataset of 424 manually digitized symptomatic crowns (64 × 64-pixel chips, augmented with rotations) was used to train a DETReg model with a ResNet-50 backbone. Inference produced 1,974 detections in Anahawan and 5,955 in Talisayan, with an average precision of ~77%. VARI stratification revealed site-dependent specificity: detections in Anahawan were dominated by High-Moderate VARI values (99.44%), suggesting overprediction of spectrally healthy crowns, while Talisayan showed a higher proportion of Low-Negative VARI values (34.14%), consistent with chlorosis from severe infestation. Findings demonstrate that DETReg can sensitively flag candidate CSI crowns from SkySat RGB imagery, but spectral limitations of four-band data and reliance on crown texture contributed to false positives and reduced transferability across landscapes. Expanding labeled samples, integrating spectral indices and temporal stacks, and applying ensemble approaches are recommended. Until validated through stratified campaigns, the method is best suited as a triage tool to prioritize ground surveys rather than for autonomous deployment.

1. Introduction

Coconut (*Cocos nucifera L.*) cultivation is a cornerstone of the nation's agricultural economy and rural livelihoods in the Philippines, supporting more than three million small farmers on over 15 million hectares of lowland and coastal lands. The industry generated export revenues of more than USD 3.2 billion in 2022 and USD 1.3 billion in 2024 (FAO, n.d.; Borres, 2024; Reyes, 2024). Beyond its substantial economic value, the coconut palm holds profound cultural significance in the Philippines, with its numerous products and by-products integral to traditional activities, handicrafts, and community-based initiatives (Carrizo, 2020). Given the coconut sector's pivotal role in the Philippine economy, the Philippine Coconut Authority (PCA) has outlined its strategic initiatives and programs for 2023 in the Trade Performance Report. Specifically, it aims to increase production, efficiency, foster value chain integration, and strengthen export competitiveness (PCA, 2023a).

Despite such developments, coconut farms and plantations remain highly vulnerable to biotic stressors, particularly the coconut scale insect (CSI; *Aspidiotus rigidus*), locally known as *cocolisap* (Figure 1a). This leaf-sucking pest, which resembles fish scales, is typically found on the underside of coconut leaves. It reproduces rapidly, multiplying every 9 days in a month (Jadina, 2014). Its feeding activity results in the secretion of honeydew, which fosters the development of sooty mold. The cumulative physiological impacts, including chlorosis (Figure 1b), leaf wilting, and diminished photosynthetic functions, can lead to tree death within six months of severe infestation (Watson et al., 2014; Serrana et al., 2019).

CSI was first reported to PCA in March 2010, signaling the onset of a rapidly expanding outbreak. It was first spotted in Barangay Balele in Tanauan, Batangas. By the time it was documented, more than 15,000 trees had already been infested within a 15-kilometer radius. PCA scientists and farmers observed serious yellowing of coconuts and the drying of the trees' leaves (Rañada, 2014). As the infestation progressed, CSI emerged as one of the most destructive pests affecting coconut production in the Philippines. This was most evident during the severe outbreak in the CALABARZON region between 2013 and 2014, which led to the death of approximately 2.1 million coconut palms and canopy defoliation rates of up to 70%. These impacts significantly contributed to yield declines and even led to social unrest (Watson et al., 2014; Cinco, 2015). The severity and extent of CSI-related damage have highlighted the pressing need for improved surveillance systems and early detection protocols.

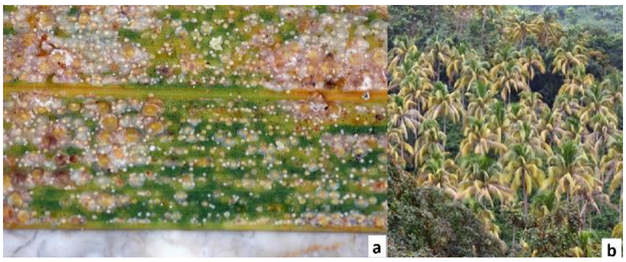

Figure 1. a) Aspidiotus rigidus, masses of adults and nymphs on a coconut leaf, and b) yellowing of mature palms caused by infestation (Shepard, M., and Carner, G., 2021).

While conventional field surveys remain essential for confirming infestations, their effectiveness is constrained by their limited spatial coverage and infrequent temporal resolution. These limitations hinder the timely identification of low-density incipient outbreaks across large coconut cultivations (Mpisane et al., 2025; Marvasti-Zadeh et al., 2022). Consequently, response strategies tend to be reactive rather than anticipatory, resulting in increased operational cost and logistical challenges in containment efforts (Parida et al., 2025; Mpisane et al., 2025).

To overcome these constraints, recent advances in geospatial technologies have introduced more scalable and proactive approaches to pest monitoring. In particular, high-resolution satellite imagery, collected at a high temporal frequency and supplemented with spectral analysis, reveals subtle physiological stress in crops, often before visible symptoms appear, thereby enabling early intervention at reduced operational costs (Mpisane et al., 2025; Marvasti-Zadeh et al., 2022; Aziz et al., 2025). Planet Labs' SkySat imagery, at 50-cm resolution, has shown promising results when processed with deep convolutional neural network (CNN) classifiers. For example, Gajbhiye et al. (2023) demonstrated early detection of pest and disease stress in rice and maize, while Kanaley et al. (2024) successfully mapped grapevine downy mildew infections in New York vineyards almost two weeks before symptoms appeared. SkySat technology has also been used in forestry to identify discolored spruce crowns from bark-beetle damage more rapidly than traditional aerial surveys (Doshi, S., 2019; Gonzalez et al., 2023).

In a foundational study, Paringit et al. (2014) employed field spectroradiometric measurements and high-resolution superspectral imagery (WorldView-2) to map spectral signatures of CSI infestation, identifying anomalies in the visible and near-infrared reflectance that consistently distinguished infested from healthy canopies. The research demonstrated the potential of fine spectral and spatial data for early detection of CSI and informed the development of remote sensing-based pest monitoring systems. The study revealed that the spectral signatures of coconuts at various degrees of infestation are fairly distinct and distinguishable in WorldView-2 satellite imagery, particularly pronounced in the NIR-1 and NIR-2 bands, and are also observed in both visible and near-infrared (NIR) regions of the electromagnetic spectrum.

To extend spectral and field-based methods toward operational monitoring, this study applied DETReg (Detection with Region Priors), a novel deep–learning object detection algorithm, to SkySat imagery to automatically detect coconut palms with CSI-related stress. DETReg can learn object localization well, even with limited amounts of annotated data, by leveraging region priors during training. It is therefore well-suited to remote sensing applications where collecting many annotated examples is difficult and expensive (Bar et al., 2022). This research implemented the approach using the ArcGIS Pro deep-learning workflow (ESRI, n.d.) and adapted the DETReg technique (Bar et al., 2022; ESRI, n.d.) to our SkySat dataset.

Building on the use of spectral indicators for vegetation health assessment, subsequent studies have explored complementary metrics such as the Visible Atmospherically Resistant Index (VARI) to enhance detection capabilities under varying illumination and atmospheric conditions. VARI, originally proposed by Gitelson et al. (2002), utilizes the red, green, and blue reflectances that improve plant signals while simultaneously reducing the effects of atmospheric conditions and illumination, making it particularly useful for RGB imagery. Unmanned Aerial Vehicle (UAV)-based studies have utilized VARI for precise mapping of coconut and oil palm health. Anisa et al. (2020) created spatially explicit maps of oil palm vigor at the Cikabayan Research Farm, Bogor City, which were strongly correlated with field-measured chlorophyll content. Nijamir and Madurapperuma (2024) utilized UAV-derived VARI in combination with deep learning approaches to map the health status of 1,597 coconut crowns in Sri Lanka at 98% accuracy.

While these earlier studies prove the efficacy of UAV-based VARI and CNN methods, none have employed this methodology on sub-meter satellite imagery for CSI detection in the Philippines. Building on these developments, this current research assesses the potential for automating CSI detection through 50-cm SkySat imagery and the DETReg deep learning technique, with VARI as an independent measure for cross-validation of canopy health status.

2. Materials and Methods

2.1 Study Sites

For this research, two primary sites were selected based on reported cocolisap outbreaks and their significance to coconut health management (Figure 2). The first site, the municipality of Anahawan in Southern Leyte, experienced a severe CSI (*Aspidiotus rigidus*) outbreak in 2020, with 5,000 coconut palms heavily infested and subjected to urgent control measures such as pruning and natural-enemy releases (Meniano, 2021; Meniano, 2023). The second site, the Philippine Coconut Authority Zamboanga Research Center (PCA-ZRC) in Barangay Talisayan, Zamboanga City, was chosen for its extensive coconut germplasm collection, and this area also faced a resurgence of cocolisap in mid-2023, where approximately 200,000 trees were attacked, prompting renewed pruning efforts and mass-rearing and release of the parasitoid Comperiella calauancia as part of targeted pest-management trials (PCA Annual Report, 2023b ; Mamac, GMA News, 2024).

Figure 2: Locations of study sites affected by reported infestations of coconut scale insects (red dots).

2.2 Materials

2.2.1 Planet SkySat Data: SkySat operated by PlanetLabs, is a high-resolution satellite imagery with a spatial resolution of 0.5m/ pixel and composed of 4 spectral bands (Planet, 2025). In this study, High-resolution SkySat Ortho Analytic Surface Reflectance (ortho_analytic_sr) images were obtained from Planet Explorer to capture the coconut canopies' conditions at the time of reported CSI infestation incidents.

For the Municipality of Anahawan, two adjacent scenes (20200908_015504_ssc13_u0001 and 20200908_015504_ssc13_u0002) taken on 08 September 2020 at 01:55 UTC were used to cover the entire area of interest (AOI). For Brgy. Talisayan, a single scene (20230917_012509_ssc12_u0002), taken on September 17, 2023, at 01:25 UTC, was used. The choice of images was based on the temporal closeness of acquisition dates relative to the reported period of the CSI outbreak. Where imagery of the actual event was unavailable, the nearest archived acquisition was used. The Talisayan scene was cloud-free, while the Anahawan scenes had cloud cover of 5% (ssc13_u0001) and 0% (ssc13_u0002), respectively (Table 1).

Area of Interest	Scene ID	Acquisition Date & Time (UTC)	Cloud Cover (%)	Projection (CRS)
Municipality of Anahawan, Southern Leyte	20200908_015504_ssc13_u0001	2020-09-08 01:55:04	5	WGS84 /UTM Zone 51N
	20200908_015504_ssc13_u0002	2020-09-08 01:55:04	0	WGS84 /UTM Zone 51N
PCA-ZRC, Brgy. Talisayan, Zamboanga City	20230917_012509_ssc12_u0002	2020-09-17 01:55:04	0	WGS84 /UTM Zone 51N

Table 1. SkySat scenes used in the study.

2.2.2 ArcGIS Pro and QGIS: ArcGIS Pro (v3.4) was utilized for pre-processing the SkySat images, generating false color composites, training, and deploying deep learning object detection models for this research. ArcGIS Pro 3.4 is a commercial desktop GIS application software for geoprocessing, spatial data analysis, and visualization. It supports advanced raster operations, machine learning, and deep learning workflows through its integration with Python (ArcPy) and frameworks such as TensorFlow and PyTorch. Additionally, QGIS (v3.28.9-Firenzze) is an open-source geographic information system used for spatial data analysis and processing. It has raster and vector functionality, geostatistics, and cartographic visualization. QGIS was also utilized in this study to calculate the VARI from SkySat imagery, create buffer zones, execute zonal statistics, and perform validation analyses to measure the accuracy of the deep learning detection outcomes.

2.2.3 Hardware Requirements: The deep learning process was performed on a workstation equipped with an Intel Core i9-13900K CPU, NVIDIA RTX 4090 GPU (CUDA enabled), 64 GB of RAM, and Windows 11 (64-bit) operating system. GPU acceleration was used to accelerate training and inference on high-resolution imagery.

2.3 Preprocessing

All imageries were orthorectified and retained at their native ground sampling distance (GSD) of 0.5 meters, georeferenced to the World Geodetic System 1984 (WGS84) datum, and projected to the Universal Transverse Mercator (UTM) Zone 51N coordinate reference system (EPSG:32651). Mosaicking was required only in the Anahawan AOI, where the two overlapping scenes were seamlessly combined in ArcGIS Pro (v3.4). Seamlines were automatically generated and then manually reviewed to ensure even radiometric consistency across the mosaic.

No additional atmospheric or radiometric corrections were executed beyond those already incorporated in the ortho_analytic_sr product, which has already taken into consideration factors such as scattering, aerosols, ozone, and water vapor through MODIS atmospheric inputs coupled with traditional atmospheric models (Planet, 2025). The final analysis was conducted at the native 0.5-meter GSD without resampling or reprojection. Due to the lack of cloud-free acquisitions near the CSI event dates, no explicit masking of non-vegetation or shadows was performed, and image interpretation proceeded on the available corrected scenes.

To differentiate potentially infested palms visually, NIR-Red-Green band false-color composites were created for the two research sites (Figures 3b and 3d). Healthy vegetation exhibits strong near-infrared reflectance and high red absorption, appearing bright red in composite images, whereas stressed vegetation displays low near-infrared reflectance and disturbed red-green ratios (NASA, n.d.).

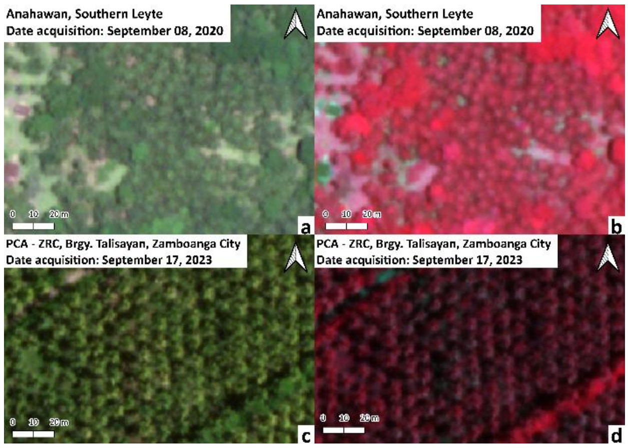

Figure 3. Suspected CSI infected palms appearance in RGB Color (a and c) and NIR-R-G False Color Composites (b and d) in the two study sites.

These spectral responses are consistent with the findings of Paringit et al. (2014), who performed field spectroradiometric measurements and WorldView-2 multispectral imagery to investigate the reflectance properties of coconut canopies of different intensities of CSI infestation. They reported significant differences along the near-infrared bands (NIR-1 and NIR-2) and red-edge region, where infested palms exhibited distinctive spectral signatures compared to healthy samples. The correlation between field spectroscopy and high-resolution satellite images suggests that CSI-induced spectral changes can be a reliable indicator of infestation. Building on this evidence, the use of NIR-Red-Green composites provided a well-founded basis for identifying suspected CSI-affected palms in SkySat imagery, which were subsequently delineated as training and reference data for model development.

2.4 Training Sample and Image Chips Preparation

Manual interpretation of the false-color composite was subsequently used to delineate coconut crowns suspected of CSI infestation from discoloration patterns, reduced near-infrared reflectance, and crown thinning. There were 424 digitized palm crowns delineated as circular vector footprints (Figure 4) in Anahawan, each of which approximated the actual canopy extent.

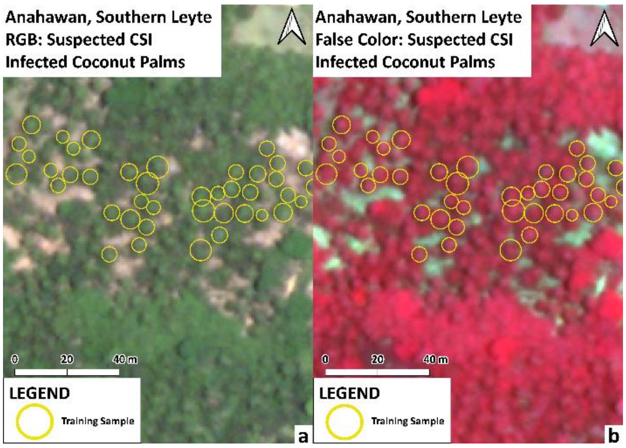

Figure 4. Suspected CSI-infected coconut trees in Brgy. Anahawan shown in a) RGB and b) false-color composites.

The marked footprints were used as input for ArcGIS Pro's Export Training Data for Deep Learning capability. Image patches or "chips" were cropped to 64 x 64 pixels in RGB. A stride of 32 pixels was applied to generate overlapping tiles, allowing the use of context information surrounding each crown. Data augmentation was performed to reduce directional bias and enlarge the effective size of the dataset through rotation at 30°.

2.5 Constructing and Inferring Deep Learning Models

In this study, the DetReg object detection model (Bar et al., 2021) was used, which combines self-supervised representation learning and a ResNet-50 convolutional backbone for the goal of enhancing generalization in low-training-data settings. The model was trained for over 100 epochs with a batch size of 8, and a 90% training and 10% validation split, utilizing an NVIDIA GPU for the sake of computation speed. The training goal was to detect and classify CSI-impacted coconut crowns from RGB inputs.

Inference was executed on the orthorectified RGB mosaic with the detection parameters as follows:

a. Confidence threshold: 0.5 (to balance precision and recall);
b. Padding: 16 pixels on all detections (to cover the entire canopy); and
c. Non-Maximum Suppression (NMS) overlap threshold: 0.1 (to discard duplicates of the same crown)

The resulting predictions were exported as ESRI shapefiles containing the geographic coordinates and bounding geometries of each palm detected.

2.6 Spectral Index Calculation, Buffer Zone Creation, and Zonal Statistics

To independently assess the palm canopy, the Visible Atmospherically Resistance Index (VARI) was derived from SkySat surface reflectance values in QGIS. VARI reduces atmospheric and illumination effects by emphasizing green reflectance relative to red and blue bands (Gitelson et al., 2002; Anisa et al., 2020; Kerezsi et al., 2024) and is given by:

$$VARI = \frac{G-R}{G+R-B}, \tag{1}$$

where *R, G,* and *B* represent the respective SkySat surface reflectance values in the red, green, and blue bands. VARI helps detect CSI-infested coconut palm trees by highlighting vegetation stress in RGB imagery. It enhances canopy greenness, reducing atmospheric effects, making early damage more visible. As a spectral feature, it improves classification accuracy in models distinguishing healthy from infested crowns. Following the spectral index calculation, centroids were extracted from the coconut trees detected as infected by CSI through the deep learning algorithm. A 3-meter buffer was then generated around each centroid to approximate the spatial extent and general shape of individual canopies. This approach was adapted from ESRI's palm tree mapping workflow of Maitoza, C. (2022).

Subsequently, zonal statistics were computed for each buffer polygon. The Zonal Statistics tool iteratively processes each polygon, identifies all VARI pixels contained within it, and calculates the mean VARI value representative of the corresponding coconut canopy. To facilitate interpretation, the resulting average VARI values were classified into four categories based on the threshold ranges (Table 2) in the papers of Gitelson et al. (2002) and Kerezsi et al. (2024), thereby allowing differentiation of canopy conditions among the detected trees.

VARI Type	VARI Values	Interpretation	Example
High VARI	**0.3–0.8**	Strong vegetation signal, high reflectance in the green band, combined with low reflectance in the red band.	Areas of dense, healthy green vegetation (e.g., forests or vigorous crop fields).
Moderate VARI	**0.1–0.3**	Some green vegetation is present, but less dense or less healthy than zones with higher VARI.	Scattered or patchy vegetation such as shrubs or crops of moderate vigor.
Low VARI	**0.0–0.1**	Suggests sparse or stressed vegetation and may also reflect non-vegetated ground like bare soil.	Typical of grasslands, low-cover areas, or vegetation experiencing stress.
Negative VARI	**-1.0–0.0**	Negative VARI values generally indicate non-vegetated surfaces; similar reflectance across the red, green, and blue bands yields low or negative values.	Bare soil, built environments, water bodies, or areas with very little vegetation.

Table 2. VARI threshold ranges from the studies of Gitelson et al. (2002) and Kerezsi et al. (2024).

This study integrates high-resolution SkySat imagery with deep learning to automate the detection of coconut scale insect (CSI) infestations (Figure 5). Ortho-analytic surface reflectance data were processed into NIR–Red–Green composites to generate training samples. RGB image chips were extracted to train an object detection model, which identified CSI-affected crowns. In parallel, the Visible Atmospherically Resistant Index (VARI) was computed to assess canopy greenness. Zonal VARI statistics were derived using a 3-meter buffer around detected crowns to evaluate individual tree condition. Combined outputs supported outbreak severity assessment.

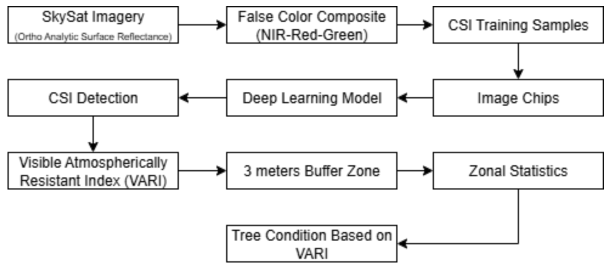

Figure 5. Workflow for detecting coconut scale insect (CSI) infestations using SkySat imagery, deep learning, and VARI-based tree condition assessment.

3. Results

The DetReg-based object detection pipeline (ResNet-50 backbone, learning rate = 2.0 x 10-5) achieved an average precision of approximately 77% for the target class of infested trees, indicating that the model attains reasonably strong precision-recall performance across detection score thresholds. The training and validation loss curves (Figure 6) show a steady decline in both losses with close tracking between the two curves throughout the training, stabilizing in the later stages. The small gap between training and validation loss indicates stable learning and no obvious severe overfitting under the chosen configuration, although loss flattening suggests diminishing returns from further training with the current dataset and hyperparameters.

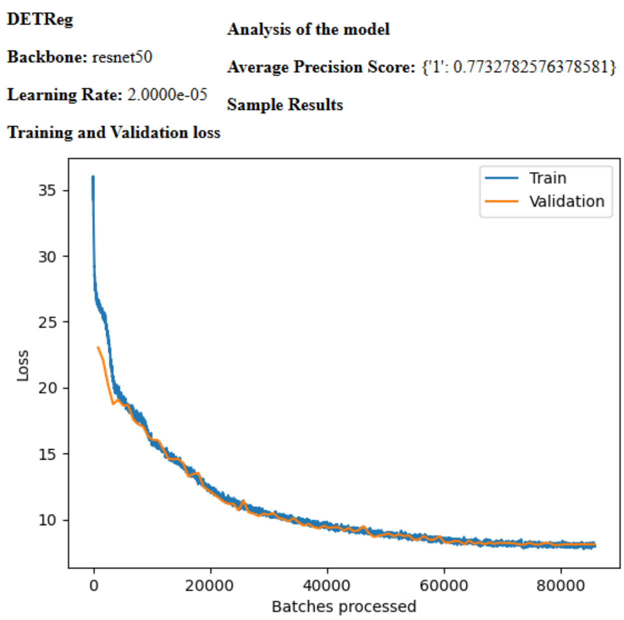

Figure 6. DETReg training and validation loss curves for Anahawan.

When applied to the two study areas, the detector flagged 1,974 suspected infested trees in Anahawan and 5,955 in Talisayan (Table 3). Taken together with the VARI cross-tabulation above (Table 2), these results indicate that, despite a good average precision score, the detector behaves in a highly sensitive manner (many candidate detections) with site-dependent specificity. In Anahawan, the large fraction of detections in the High (56.94%) and Moderate (42.50%) VARI classes, and negligible Low (0.56%) and Negative (0%) coverage, implies a high false positive rate in that landscape, which indicates that spectrally healthy canopies are being flagged. In contrast, detections in Talisayan show a VARI distribution shifted toward lower classes (High VARI = 0.82%, Moderate VARI = 65.04%, Low VARI = 19.82%, and Negative VARI = 14.32%), producing a combined Low-Negative share of 34.14% that qualitatively matches expected chlorosis from heavy CSI pressure but still leaves a majority of detections in High-Moderate VARI. Thus, while the average precision shows the model is effective at discriminating candidate objects overall, the site-level VARI comparison demonstrates reduced specificity in stands with only moderate or subtle symptoms and highlights substantial over-prediction in some landscape contexts.

Study Area	**Total detections (n)**	**High VARI (%) / (n)**	**Moderate VARI (%) / (n)**	**Low VARI (%) / (n)**	**Negative VARI (%) / (n)**
Anahawan	1,974	56.94% / 1,124	42.50% / 839	0.56% / 11	0.00% / 0
Talisayan	5,955	0.82% / 49	65.04% / 3,873	19.82% / 1,180	14.32% / 853

Table 3. Table showing VARI-class percentages (%) and counts (n) for Anahawan and Talisayan, with Anahawan dominated by High-Moderate VARI and Talisayan showing a larger Low-Negative share.

Maps of the deep-learning model outputs for the two study areas, Anahawan in Southern Leyte (Figure 7), and PCA-ZRC Talisayan in Zamboanga City (Figure 8), reveal different spatial patterns that help explain the site-dependent specificity noted above.

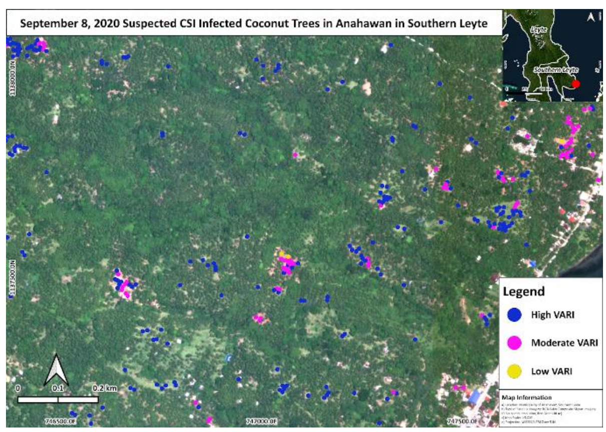

Figure 7. Detected CSI-coconut trees using DETReg object detection and their corresponding VARI values in Anahawan, Southern Leyte, on September 8, 2020.

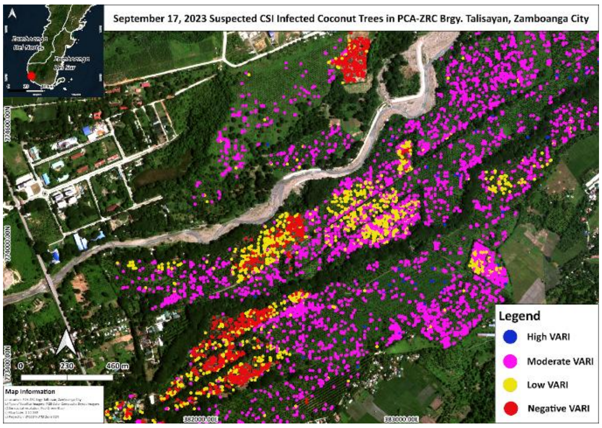

Figure 8. Detected CSI-coconut trees using DETReg object detection and their corresponding VARI values in PCA-ZRC Brgy. Talisayan, Zamboanga City, on September 17, 2023.

These combined findings suggest that the deep learning model in Anahawan is well-trained in the sense of convergent loss and a solid average precision metric, but it is tuned toward sensitivity at the expense of precision in certain canopy conditions.

4. Discussion

4.1 Key Findings

Application of DETReg to 0.5-meter SkySat imagery produced a detector with an overall average precision of ~77% with an extremely high candidate detection rate (1,974 in Anahawan; 5,955 in Talisayan). VARI-based cross-tabulation displayed significant site differences: Anahawan detections predominantly in High-Moderate VARI (High = 56.94%; Moderate = 42.50%) classes, while Talisayan detections were higher in Low-Negative VARI (combined percentage of 34.14%). These patterns indicate the model is highly sensitive to palm crown features, but the spectral confirmation (VARI) demonstrates variable specificity by landscape condition and outbreak severity.

4.2 Interpretation: Sensitivity versus Specificity

The model's behavior reflects two complementary effects. First, spatial sampling of high-resolution SkySat imagery enables precise crown localization, increasing the detection based on textural and morphological features. Second, the low spectral dimensionality of SkySat (broad-band RGB/NIR) constrains the ability to distinguish subtle or localized physiological stress. Consequently, the detector tends to flag visually or texturally anomalous crowns where VARI does not indicate chlorosis, specifically in areas like Anahawan, resulting in false positives. In contrast, in areas like Talisayan, where chlorosis is widespread and more evident, detections more closely align with low VARI values. Overall, the pipeline demonstrates high sensitivity in generating candidate detections but requires additional spectral, temporal, or contextual inputs to improve precision.

4.3 Sources of Errors and Transferability Limitations

False positives are likely caused by confounding canopy textures such as pruning, mechanical injury, senescing fronds, variations in shadowing and illumination effects, simultaneous abiotic or other biotic stress, and potential label noise in the training dataset. False negatives continue to pose challenges, particularly for early-stage or inner-canopy infestations that are spectrally subtle from nadir views. The contrasting site results indicate limited direct transferability. Models learned on one landscape or phenological stage may over- or under-predict in other contexts without retraining or domain adaptation.

4.4 Limitations

Key limitations include the limited size and potential label noise in the training dataset (n = 424 labeled crowns), the limited spectral richness of SkySat ortho_analytic_sr, and the single-date imagery dependence per study area. VARI is a coarse, qualitative indicator of chlorophyll content; thus, it cannot substitute for field-based biochemical measurements. Finally, the current evaluation uses average precision as a global summary, but more granular metrics such as (stratified confusion matrices, and class-wise recall) are needed to fully characterize model performance across varying levels of symptom severity. Field validation (in-situ surveys) is also required to verify detection results and to confirm the correspondence between VARI and ground-survey observations.

4.5 Practical Implications

With the current capability, the combination of DETReg and SkySat is most useful as an operational triage tool. It could potentially reduce the required human inspection by marking high-priority candidate crowns and clusters for on-the-ground verification. Utilizing these detections for directed surveys can accelerate response to outbreaks and optimize resource utilization. However, rigorous on-the-ground verification and conservative operational threshold criteria must be established before delegating management decisions to the model.

4.6 Recommendations to Improve Robustness

To enhance model generalization and reduce bias, the training dataset should be expanded and diversified to include validated training samples that represent the full range of infestation severities, canopy structures, planting densities, and non-CSI stressors (e.g., nutrient stress, drought, and pruning impacts). Coupling this enhanced dataset with active learning and targeted field sampling can significantly improve labeling efficiency. Specifically, model uncertainty can be used to prioritize ground verification at borderline detections and high uncertainty regions, as these samples tend to yield the greatest performance gains per unit field effort. Additionally, field validation should also be embedded in the workflow to ensure that detection outcomes and vegetation index signals consistently align with on-the-ground conditions.

Supplementing multi-channel inputs and derived features will help the detector distinguish true physiological stress from purely textural anomalies. Specifically, supply the network with spectral indices as VARI and, where available, Normalized Difference Vegetation Index (NDVI) or Green Chlorophyll Index (GCI) as auxiliary channels, and incorporate texture statistics or band ratios as model inputs or as a post-classification filter. These additional data layers can anchor shape- and texture-based detection to the spectral indicator of chlorosis and increase specificity.

Temporal analysis is another important pathway: integrating multi-date imagery and simple change detection statistics, it is possible to identify slow chlorosis and crown decline, enabling the model to separate persistent CSI signals from transient shadows or seasonal variation. Additionally, algorithmic strategies, e.g., ensembles and hybrid workflows that combine object detection approaches with pixel-wise or object-wise classifiers, are able to reduce system error and variance by combining multiple viewpoints on the same data. Finally, strict and stratified evaluation practices (precision, recall, F1 score, Intersection over Union (IoU), Precision-Recall curves), by VARI class, canopy density, and date of acquisition, are necessary to reveal failure modes and directly guide future model development.

5. Conclusion

This study demonstrates that a DETReg object detector applied to 0.5 m SkySat imagery can sensitively identify candidate coconut crowns exhibiting spatial patterns consistent with CSI damage characteristics. The processing system yielded a promising mean average precision of around 77% and delivered spatially explicit maps of detection for the two outbreak sites. However, VARI cross-validation revealed site-specific variability in specificity, including a notable bias towards false positives in some landscapes and stronger spectral alignment in others with extensive chlorosis. These results suggest that high-resolution satellite images can play a significant role in landscape-scale CSI monitoring, but single-date RGB/NIR detection alone is not sufficient for fully autonomous operational use. To move towards successful monitoring, the methodology must be strengthened by expanding and diversifying labeled datasets, incorporating auxiliary spectral and temporal information, applying active learning to refine annotations, and combining detectors with spectral classifiers or ensembles. In the next few years, the most practical deployment is as a triage system that prioritizes areas and trees for targeted field inspection, thereby increasing the efficiency of ground surveys and control efforts. With these enhancements and rigorous, stratified field validation, SkySat-based deep learning approaches hold immense potential as a component of national CSI surveillance and rapid-response systems for the Philippines' coconut industry.

6. References

Anisa, M. N., Rokhmatuloh, N., Hernina, R. 2020: UAV application to estimate oil palm trees health using Visible Atmospherically Resistant Index (VARI) (case study of Cikabayan Research Farm, Bogor City). E3S Web of Conferences, 211, 05001. https://doi.org/10.1051/e3sconf/202021105001

Aziz, D., Rafiq, S., Saini, P., 2025: Remote sensing and artificial intelligence: revolutionizing pest management in agriculture. *Front. Sustain. Food Syst.,* 9, 1551460. https://doi.org/10.3389/fsufs.2025.1551460.

Bar, A., Wang, X., Kantorov, V., Reed, C. J., Herzig, R., Chechik, G., Rohrbach, A., Darrell, T., Globerson, A., 2021: DETReg: Unsupervised pretraining with region priors for object detection. *arXiv*. https://doi.org/10.48550/arXiv.2106.04550.

Borres, I. L., 2024: Industry analysis of coconut businesses in the Philippines. *ISRG J. Econ. Bus. Manag.,* II (6), 114–115. https://doi.org/10.5281/zenodo.14353493.

Carrizo, A. L., 2020: Coconut farming in the Philippines. Producers Stories. Available at: https://producersmarket.com/blog/coconut-farming-in-the-philippines/ (accessed 29 May 2025).

Cinco, M., 2015: Agency warns of return ‘cocolisap’. *Inquirer News*. Available at: https://newsinfo.inquirer.net/690673/agency-warns-of-return-of-cocolisap (accessed 29 May 2025).

Doshi, S., 2019: Bark beetles are decimating forests: satellite data can help. Planet Pulse, 3 Sept 2019. Available at: https://www.planet.com/pulse/bark-beetles-are-decimating-forests-satellite-data-can-help/ (accessed 29 May 2025).

ESRI. n.d.: Detecting palm trees using deep learning | ArcGIS API for Python. Available at: https://developers.arcgis.com/python/latest/samples/detecting-palm-trees-using-deep-learning/ (accessed 29 May 2025).

Food and Agriculture Organization of the United Nations (FAO), n.d.: Restoring coconut farmers’ livelihoods in the Philippines. Available at: https://www.fao.org/in-action/restoring-coconut-farmers-livelihoods-in-the-philippines/en/ (accessed 29 May 2025).

Gajbhiye, M., Agrawal, K. K., Jha, A. K., Kumar, N., Raghuwanshi, M., 2023: Crop health monitoring through remote sensing: a review. *Int. J. Environ. Clim. Change,* 13(10), 2581–2589. https://doi.org/10.9734/ijecc/2023/v13i102924.

Gitelson, A. A., Stark, R., Grits, U., Rundquist, D., Kaufman, Y., Derry, D. 2002: Vegetation and soil lines in visible spectral space: A concept and technique for remote estimation of vegetation fraction. *International Journal of Remote Sensing*, 23(13), 2537-2562. https://doi.org/10.1080/01431160110107806.

Gonzalez, J., Straub, C., Seitz, R., Felten, B., Schauer, P., 2023: Damage to spruce trees: what satellite technology can capture. Waldwissen. Available at: https://waldwissen.net/en/forestry/forest-protection/damage-to-spruce-trees-what-satellite-technology-can-capture/ (accessed 29 May 2025).

Jadina, M., 2014: Saving the PH coconut industry. Philippine Institute for Development Studies (In the News). Available at: https://pids.gov.ph/details/saving-the-ph-coconut-industry (accessed 29 May 2025).

Kanaley, K., Combs, D. B., Paul, A., Jiang, Y., Bates, T., Gold, K. M., 2024: Assessing the capacity of high-resolution commercial satellite imagery for grapevine downy mildew detection and surveillance in New York State. *Phytopathology*. https://doi.org/10.1094/PHYTO-11-23-0432-R.

Kerezsi, G., Kun, Á., Jancsó, M., 2024: Examination of red clover optimum harvesting status in seed production with unmanned aerial systems (UAS). *J. Cent. Eur. Green Innov.,* 12(3), 3–19. https://doi.org/10.33038/jcegi.6437.

Maitoza, C., 2022: Use deep learning to assess Palm Tree health (tutorial). ArcGIS StoryMaps, 21 April 2022. Available at: https://storymaps.arcgis.com/stories/125c7ad83e40490d9965611c3dfec31e (accessed 29 May 2025).

Mamac, E. Y., 2024: “Cocolisap” infests coconut trees in Zamboanga Peninsula. GMA Regional TV, 26 Jan 2024. Available at: https://www.gmanetwork.com/regionaltv/news/100255/cocolisap-infests-coconut-trees-in-zamboanga-peninsula/story/ (accessed 29 May 2025).

Marvasti-Zadeh, S. M., Goodsman, D., Ray, N., Erbilgin, N., 2022: Early detection of bark beetle attack using remote sensing and machine learning: a review. *arXiv*:2210.03829. Available at: https://arxiv.org/abs/2210.03829 (accessed 29 May 2025).

Meniano, S., 2021: PCA contains coco pest in Southern Leyte. Philippine News Agency. Available at: https://www.pna.gov.ph/articles/1136113 (accessed 21 August 2025).

Meniano, S., 2023: PCA shuns the lifting of the coco transport ban in Southern Leyte town. Philippine News Agency, 9 March 2023. Available at: https://www.pna.gov.ph/articles/1196995 (accessed 29 May 2025).

Mpisane, K., Kganyago, M., Munghemezulu, C., Price, R., Nduku, L., 2025: A systematic review of remote sensing technologies and techniques for agricultural insect pest monitoring: lessons for *Locustana pardalina* (brown locust) control in South Africa. *Front. Remote Sens.,* 6, 1571149. https://doi.org/10.3389/frsen.2025.1571149.

NASA Earth Observatory, n.d.: Why is that forest red and that cloud blue? Available at: https://earthobservatory.nasa.gov/features/FalseColor/ (accessed 29 May 2025).

Nijamir, K., Madurapperuma, B. D. 2024: Detecting and Mapping Individual Coconut Tree Crowns Using Deep Learning from UAV Imagery at the Oluvil Coastal Fringe in Ampara District, Sri Lanka. Proceedings of the 28th International Forestry and Environment Symposium 2024, University of Sri Jayewardenepura, Sri Lanka.

Parida, P., Longkumer, I. Y., Devi, Y. K., 2025: Remote sensing and GIS: important tools for agricultural insect pest monitoring. *Int. J. Adv. Biochem. Res.,* SP-9(4), 30–35. https://doi.org/10.33545/26174693.2025.v9.i4Sa.4045.

Paringit, E. C., Cruz, C., Fabila, J. L. D., Samalburo, S., 2014: Spectral characterization of coconut scale insect (CSI) from field spectroradiometric measurements and high-resolution superspectral imagery. Available at: https://www.researchgate.net/publication/286634102 (accessed 29 May 2025).

Philippine Coconut Authority (PCA), 2023a: Narrative and trade performance reports. Available at: https://pca.gov.ph/index.php/trade-market/trade-performance/narrative-and-trade-performance-reports (accessed 29 May 2025).

Philippine Coconut Authority (PCA), 2023b: PCA Annual Report 2023: Half a Century Journey — 50th Year of Heartfelt Service. Philippine Coconut Authority, Quezon City, Philippines. Available at: https://pca.gov.ph/images/pdf/annualreport/PCA_Annual_Report_2023.pdf (accessed 29 May 2025).

Planet, 2025: SkySat. Planet Documentation, 21 July 2025. Available at: https://docs.planet.com/data/imagery/skysat/ (accessed 29 May 2025).

Rañada, P., 2014: New pest fast destroying coconut trees in Luzon. Rappler. Available at: https://www.rappler.com/nation/49333-coconut-scale-infestation-luzon (accessed 29 May 2025).

Reyes, M. A. L. 2024: Tree of life. PhilStar Global, 15 September 2024. Available at: https://www.philstar.com/business/2024/09/15/2385270/tree-life (accessed 29 May 2025).

Serrana, J. M., Ishitani, N., Carvajal, T. M., Almarinez, B. J. M., Barrion, A. T., Amalin, D. M., Watanabe, K., 2019: Unraveling the genetic structure of the coconut scale insect pest (*Aspidiotus rigidus* Reyne) outbreak populations in the Philippines. *Insects*, 10(11), 374. https://doi.org/10.3390/insects10110374.

Shepard, M., Carner, G., 2021a: Masses of adults and nymphs of the coconut (false) scale, *Aspidiotus rigidus*, on the leaf of a coconut [photograph]. *Pacific Pests, Pathogens & Weeds (PPPW)* Online edition: Jackson, G. Coconut (false) scale (348). Available at: https://apps.lucidcentral.org/pppw_v10/text/web_full/entities/coconut_false_scale_348.htm (accessed 20 August 2025).

Shepard, M., Carner, G., 2021b: Yellowing of mature palms due to infestation of coconut (false) scale, *Aspidiotus rigidus* [photograph]. *Pacific Pests, Pathogens & Weeds (PPPW)* Online edition: Jackson, G. Coconut (false) scale (348). Available at: https://apps.lucidcentral.org/pppw_v10/text/web_full/entities/coconut_false_scale_348.htm (accessed 20 August 2025).

Watson, G. W., Adalla, C. B., Shepard, B. M., Carner, G. R., 2014: *Aspidiotus rigidus* Reyne (Hemiptera: Diaspididae): a devastating pest of coconut in the Philippines. *Agric. For. Entomol.,* 17, 1–8. https://doi.org/10.1111/afe.12074.